Article

Empowering Design Based on Hybrid Twin^TM: Application to Acoustic Resonators

Clara Argerich Martín [1,2,*], Arnulfo Carazo Méndez [3], Olivier Sainges [3], Emilie Petiot [1], Anais Barasinski [4], Mathieu Piana [1], Louis Ratier [3] and Francisco Chinesta [2]

[1] Airbus Group, Rue de l'Aviation, 44340 Bouguenais, France; emilie.petiot@airbus.com (E.P.); mathieu.piana@airbus.com (M.P.)

[2] PIMM Lab, Arts et Métiers Institute of Technology 151 Boulevard de l'Hôpital, 75013 Paris, France; Francisco.Chinesta@ensam.eu

[3] Airbus Group, 26 Chemin de l'Espeissière, 31300 Toulouse, France; arnulfo.carazo-mendez@airbus.com (A.C.M.); olivier.o.sainges@airbus.com (O.S.); louis.ratier@airbus.com (L.R.)

[4] Université de Pau et des Pays de l'Adour, E2S UPPA, CNRS, 64000 Pau, France; anais.barasinski@univ-pau.fr

[*] Correspondence: clara.argerich_martin@ensam.eu

check for updates

Abstract: In the framework of civil aviation noise levels are becoming restricted every year, on one hand to provide comfort to the passengers and on the other hand to be compliant with regulations protecting airports surroundings. New technologies are required to reduce noise to cope with this restrictions as well as to guarantee a comfortable flight for passengers. For technological industries it is compulsory to stay competitive and keep improving the technology related to air intake acoustic liners. With an unceasingly growing market, for industries it is key to stay in the vanguard of air inlet technologies, ensuring innovation and establishing a proactive environment for future product generations. One of the main objectives in this framework is the reduction of the development time of these new technologies in all the stages of the process. In this work we focus on the design stage of a new prototype and we propose a hybrid technique enabling faster design and the reduction of development time. When designing new technologies or prototypes there are usually two constraints. On one hand, more innovative prototypes may present unconventional shapes are not accurately represented by conventional physical models. On the other hand, the available data is scarce, thus limiting the use of most innovative techniques based on the state-of-art of Artificial Intelligence. In this paper we propose a solution laying in the hybrid twin paradigm, combining both, data in the low limit and physics to provide a hybrid model able to represent unconventional and innovative acoustic solutions.

Keywords: hybrid twin; digital twin; acoustic resonator; low-data; fast design

1. Introduction

Innovation in industry is a key factor for competitiveness in the market. In order to empower competitiveness industries need to implement new technologies, optimize the existing ones while addressing changing requirements. In general terms, the implementation of a new technology goes through the following stages: conceptual design, first tests with numerical simulations, prototype design, experiments on the prototypes and final design. The aim of this paper is to present a hybrid technique enabling the engineer to make decisions with a reduced number of built prototypes, thus reducing the development time of new technologies. For that purpose the development of a new acoustic technology in aviation is going to be used as an example to display the benefits of using a dual data-physics engineering approach.

Technology concerning noise absorption in aviation is continuously being improved in order to provide comfort for passengers and be compliant with the legislation (see [1]). For keeping up with the restrictions new and innovative technologies are constantly being studied, different examples can be found in [2–4]. In this paper we focus on the acoustic absorption taking place in the nacelle of an aircraft, that is the part surrounding the fan. To establish a clear context, Figure 1 depicts on the left side an aircraft nacelle with an area of the acoustic liner highlighted in red, on the right image, a schematic visualization of the technology being currently used by most manufacturers for the acoustic liners is sketched. The adopted technology consists of a layer composed by perforated composite, a metallic wiremesh followed by a honeycomb structure and a back skin to provide rigidity.
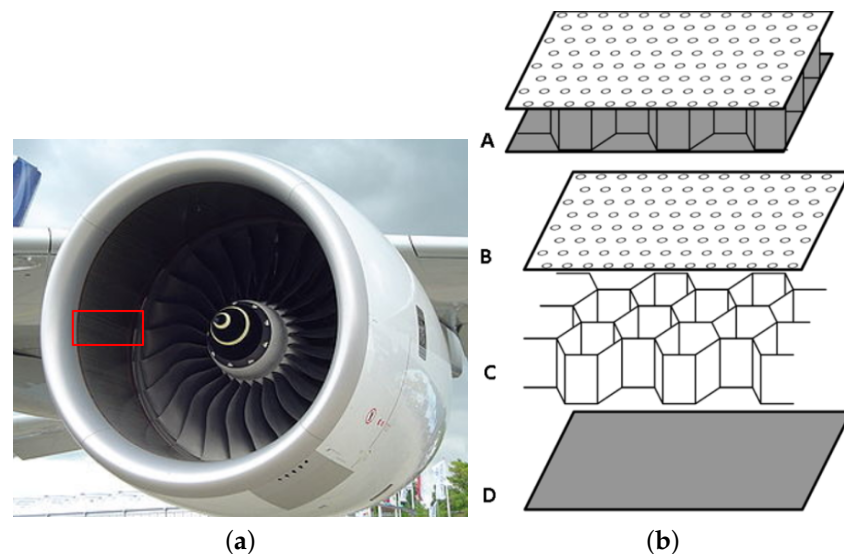

| (a) | (b) |

Figure 1. Nacelle and Acoustic Conventional Liner.

In pursuance of improvement in acoustic liners, new designs different from Figure 1 are currently being explored. The analysis of acoustic resonators depends on strong hypotheses and there is currently a vast literature on the topic. In general acoustic liners can be analyzed both, in the time and in the frequency domain, involving each one different methods compiled in [5] and here grouped in Table 1, where the impedance is the quantity of interest, defined as the ratio between the acoustic pressure and air velocity normal to the locally reacting wall.

Table 1. Global Vision of analysis of acoustic liners; frequency domain vs. time domain.

	Frequency Domain (w)	**Time Domain (t)**
Impedance	Z(w) is a boundary condition	Z(w) comes from a model
Uses	Low computational effort Fast and accurate solutions	Broadband Noise Non-linear problems Non-sationary background flows
Methods	Use of full viscous acoustics	Experimental studies Linear acoustics Not full viscous acoustics Computationally expensive

The follow-up for the digital resolution of an acoustic coating problem is: (i) defining the boundary conditions by selecting an impedance value in the locally reacting wall, (ii) solve the sound propagation and (iii) check the assumed boundary condition. First, the boundary conditions, i.e., the impedance of a locally reactive wall, must be assumed. There are several models to be applied depending on the selected hypothesis, as presented in [6] one could use the most basic models: Pridmore-Brown,

the Myers model (valid for an infinitely thin boundary layer), the Möhring model (valid for a rotational flow) and the convective wave equation (valid for an irrotational flow) among many others. In [7] numerical tools to solve sound propagation in acoustic liners are reviewed, starting from the Navier-Stokes equations [5], very accurate but expensive from the computational viewpoint to some reduced formulations that even that are less accurate, they are computationally more efficient. The suppression of the diffusive term in the Navier-Stokes equations leads to the linearized Euler equations [8,9] and finally the Helmholtz equation implies the use of the hypothesis of a hometropic and irrotational flow. Finally, a check of the boundary condition can be performed. In summary, it is necessary to define the boundary conditions of an acoustic liner (usually using the Myers model or in a laboratory according to ISO10835-2), then solve the problem of sound propagation (linearized Euler equations are the most common in the bibliography) and finally verifying the boundary condition using experimental or reference data.

On the other hand, alternative methods based on empirical equations or equivalences are also used to validate acoustic coatings. One of the most common models for evaluating the local impedance of an asset is electro-acoustic equivalence, in which an acoustic system is replaced by an electrical system, or mass-spring equivalence usually used in the low-frequency range as shown in [10,11] or for real-time solutions, as proven in [4].

Methods based on empirical or semi-empirical relations are widely used in industry, particularly in the early stages of designing new prototypes, because they provide very rapid responses. The formulas are adapted to different conditions, for example, in [12], different models are presented, from Maa's model for local reaction ships to the Kirby and Cumming's model or the Kooi and Sari's model, both taking into account the grazing flow. A comparative analysis of the different models can be found in [13].

Finally, the Guess model presented in [14] should be highlighted. This empirical model for the calculation of the perforated sheet metal coating takes into account viscosity, support effects and non-linearities present in the term due to the high sound amplitude and constant tangential air flow.

However, new designs may be unconventional from a classical point of view, thus narrowing the use of empirical models built for well-known acoustic solutions or liners. The development of new acoustic liners goes through the following steps: design a new prototype, manufacture different samples, and evaluate them at a primary level for then fabricating them at industrial scale to perform the final evaluation. When subsequently developing a new acoustic technology, current empirical physical models may not be enough to predict actual sound absorption due to multiple facts, much as the different hypothesis required by models. As a result, many experimental tests are required, which leads to a long development time and increased costs.

The aim of this paper is to validate a methodology that relies on the existence of predictive models as a tool to minimize the drawbacks of choosing empirical models or solutions involving high computational cost. The use of predictive models implies a reduction on the sample prototypes necessary for assessing a final design. The fact that we found ourselves in a low-data framework, such as the development of new technologies limited by the number of samples manufactured, limits the use of standard learning techniques that pave the AI framework. To cope with this whole scenario we propose a hybrid solution. This kind of approach combines knowledge gathered in a physical model enriched from data. The strong point of hybrid modeling resides on the modeling of non-linearities. Acoustics around maximum absorption frequency is often led by non-linear phenomena, thus making it difficult to use of regression techniques to obtain empirical models, however, an accurate enough physics-based model it is expected capturing most of the nonlinear behavior, then the regression is only expected filling the gap between the physics-based model predictions and the measured data. The original model plus the correction leads to an accurate model combining knowledge and data while reducing the data-needs.

2. Problem Statement

The objective of this paper is to validate a hybrid methodology for the design of acoustic resonators. When a new acoustic design is required it needs to be tested and implemented within a given schedule. First samples are 3D printed at a lower scale to obtain an empirical model that will enable the final design. The acoustic behaviour of these samples is measured in an experimental campaign and from the results an empirical model is extracted. The general procedure goes as follows:

- Build samples of the acoustic prototype
- Obtain their acoustical behaviour from experiments
- Correlate the acoustical behaviour with the geometrical characteristics of the sample
- Obtain the acoustic model of the prototype

The more samples built and tested, the more accurate the model will be, however, a larger experimental set will imply more cost in both, time and resources. The methodology proposed in this paper has a direct impact on the extraction of the correlation between geometry and acoustical behaviour. The proposed methodology is a hybrid between data-driven and physical formulas. On one hand, an acoustical model will be chosen for evaluating the resonators, the information obtained by this model will be completed with a data-driven approach on the experimental data. This procedure overcomes two issues: the difficulty of choosing an acoustical model that will explain all the physical phenomena and the need of large amounts of data for performing a data-driven approach. By combining these both ingredients a hybrid-model can be obtained with a reduced number of samples. In the next sections we present the considered methodology, define the prototype geometry ad the related parameters defining it.

3. Methodology

The proposed methodology is based on an approach developed by ESI Group called Hybrid Twin^{TM}. It is a dual approach that combines physical models and data-based correction. In this scenario, data-based enrichment fills the gap between the physical models and reality. In other words, this correction will realign the virtual world with reality.

What is usually done at the design stages of new technologies is to capture the behaviour of the prototypes by means of a regression or statistical analysis. The bottleneck in this approach is the fact that the accuracy of the regression is directly related to the number of prototypes (also called data-points) used for building it. This is a key factor when designing new prototypes, because the more samples are available, the more precise the design will be, but also the development time will increase (more samples will be required to be built and tested), and the associated cost.

The interest of this hybrid approach in the context of this study lies in the nature of the new prototypes. A new prototype can be based on a well-known physical model, such as the Helmholtz resonator or the quarter wave resonator (see [15]), but due to variations or too strong hypothesis, these classical models are not sufficient to describe the resonator, whose behavior may often be found between those two models. We aim to build a model of the "gap", i.e., a model of the difference between the theoretical output and the measured output. This rationale is depicted in Figure 2.

To summarize, the requirements for performing an hybrid approach for analyzing an asset are:

1. Obtain experimental measurements of the quantity of interest.
2. Select a physics based ground-model describing the asset and the quantity of interest to observe.
3. Perform a regression on the difference of the physics-based models and the collected data, the so-called data-driven model of the deviation (representing the pre-existence ignorance).
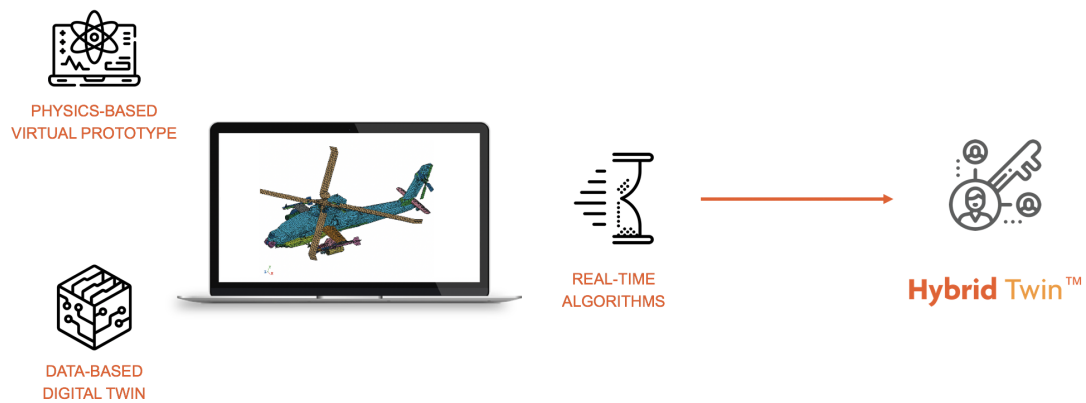
Figure 2. Hybrid modelling rationale, image courtesy of ESI group.

As in the HT the data-drive model only concerns the deviation, instead of the model itself, and being that deviation in general less nonlinear that the model itself, its construction needs much less data, improving the design in both, development time and cost.

4. Prototype Data

The case treated in this work comes from a new acoustic prototype depicted in Figure 3 This work was done in collaboration with the Airbus acoustical studies office based in Toulouse.
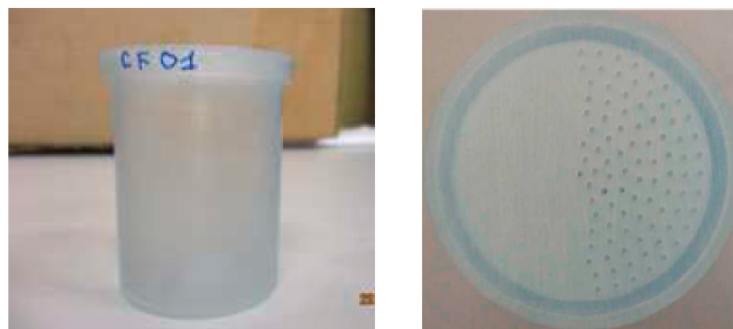

Figure 3. 3D printed prototypes for acoustic measuring bench.

A sketch of the prototype object of this study can be seen in Figure 4.
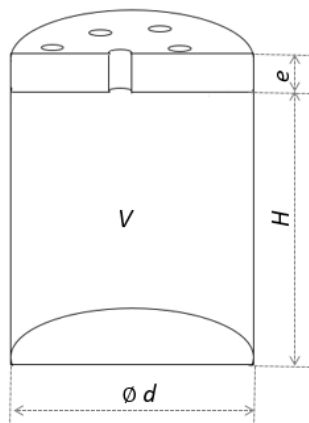

Figure 4. Sketch of the prototypes.

The following inputs were considered:

- Percentage of aperture of the cover, *POA* This parameters represents the ratio of surface holes to total surface.
- Diameter of the cylinder, *d*.
- Height of the cylinder, *H*
- Open Surface, *So*, this parameter is the sum of the area of all the orifices in the cover.
- Width of the cover, *e*
- Volume of the cavity *V*
- Theoretical resonance frequency,

In this case the quantity of interest or target was the measured resonance frequency, which is also the frequency of maximum absorption.

Concerning the dual methodology proposed in this work the resonance frequency from experiments is assumed to be equivalent to the resonance frequency from the Helmholtz model plus a correction, Equation (1).

$$\mathcal{F}_{r,data} = \mathcal{F}_{r,model} + C \tag{1}$$

where $\mathcal{F}_r$ stands for resonance frequency and C for the correction.

In the data-driven approach the regression is performed on $\mathcal{F}_{r,data}$, whereas within the Hybrid Twin rationale here proposed the regression only concerns the correction, C. The most outstanding benefit is that as mentioned, with most of non-linearities already taken into account by $\mathcal{F}_{r,model}$, the data-driven regression becomes cheaper.

4.1. Experimental Measurement

The experimental campaign concerns prototypes built with 3D printing and tested in an acoustical bench based in the normative [16]. The number of cylindrical samples used in this study is 23 and the input data collected was composed by the theoretical value of the geometrical descriptors of the asset as well as the measured value of these inputs after printing the samples. After the testing another attribute was added to the data-set, the experimental value of the resonance frequency, key for performing the hybrid approach as previously described. The geometrical data as well as the theoretical value of the resonance frequencya and the experimental one can be found in Table 2.

Table 2. Geometrical values of the prototypes along with the theoretical and experimental resonance frequencies.

e [mm]	V [m3]	So	d [m]	h [m]	Theoretical Freq [Hz]	Experimental Freq [Hz]
9.50×10^{-1}	4.81×10^{-5}	1.45×10^{-4}	1.00×10^{-3}	5.00×10^{-2}	3.08×10^3	1.38×10^3
9.80×10^{-1}	4.81×10^{-5}	9.68×10^{-5}	1.00×10^{-3}	5.00×10^{-2}	2.49×10^3	1.27×10^3
1.00×10^0	4.81×10^{-5}	7.23×10^{-5}	1.00×10^{-3}	5.00×10^{-2}	2.12×10^3	1.03×10^3
1.01×10^0	4.81×10^{-5}	4.80×10^{-5}	1.00×10^{-3}	5.00×10^{-2}	1.72×10^3	9.30×10^2
7.00×10^{-1}	4.81×10^{-5}	1.45×10^{-4}	1.00×10^{-3}	5.00×10^{-2}	3.59×10^3	1.47×10^3
1.50×10^0	4.81×10^{-5}	1.45×10^{-4}	1.00×10^{-3}	5.00×10^{-2}	2.45×10^3	1.26×10^3
1.93×10^0	4.81×10^{-5}	1.44×10^{-4}	1.00×10^{-3}	5.00×10^{-2}	2.16×10^3	1.17×10^3
9.90×10^{-1}	4.81×10^{-5}	1.44×10^{-4}	7.50×10^{-4}	5.00×10^{-2}	3.01×10^3	1.36×10^3
9.80×10^{-1}	4.81×10^{-5}	1.44×10^{-4}	1.50×10^{-3}	5.00×10^{-2}	3.03×10^3	1.36×10^3
1.00×10^0	4.81×10^{-5}	1.45×10^{-4}	2.00×10^{-3}	5.00×10^{-2}	3.00×10^3	1.25×10^3
9.90×10^{-1}	4.81×10^{-5}	7.22×10^{-5}	1.00×10^{-3}	5.00×10^{-2}	2.13×10^3	1.00×10^3

Table 2. *Cont.*

e [mm]	V [m3]	So	d [m]	h [m]	Theoretical Freq [Hz]	Experimental Freq [Hz]
9.30×10^{-1}	4.81×10^{-5}	4.81×10^{-5}	1.00×10^{-3}	5.00×10^{-2}	1.79×10^{3}	8.50×10^{2}
1.95×10^{0}	4.81×10^{-5}	1.45×10^{-4}	7.50×10^{-4}	5.00×10^{-2}	2.15×10^{3}	1.14×10^{3}
1.98×10^{0}	4.81×10^{-5}	1.45×10^{-4}	2.00×10^{-3}	5.00×10^{-2}	2.13×10^{3}	1.07×10^{3}
5.60×10^{-1}	4.81×10^{-5}	1.45×10^{-4}	7.50×10^{-4}	5.00×10^{-2}	4.01×10^{3}	1.59×10^{3}
7.20×10^{-1}	4.81×10^{-5}	1.44×10^{-4}	2.00×10^{-3}	5.00×10^{-2}	3.54×10^{3}	1.35×10^{3}
9.75×10^{-1}	9.62×10^{-5}	1.44×10^{-4}	1.00×10^{-3}	1.00×10^{-1}	2.15×10^{3}	7.50×10^{2}
9.60×10^{-1}	2.41×10^{-5}	1.45×10^{-4}	1.00×10^{-3}	2.50×10^{-2}	4.33×10^{3}	2.37×10^{3}
9.65×10^{-1}	1.51×10^{-4}	1.45×10^{-4}	1.00×10^{-3}	5.00×10^{-2}	1.72×10^{3}	8.50×10^{2}
1.04×10^{0}	2.45×10^{-4}	1.45×10^{-4}	1.00×10^{-3}	5.00×10^{-2}	1.29×10^{3}	6.25×10^{2}
1.04×10^{0}	1.51×10^{-4}	1.45×10^{-4}	1.00×10^{-3}	2.50×10^{-2}	1.59×10^{3}	8.80×10^{2}
9.47×10^{-1}	7.22×10^{-5}	1.45×10^{-4}	1.00×10^{-3}	7.50×10^{-2}	2.52×10^{3}	9.70×10^{2}
9.97×10^{-1}	2.41×10^{-5}	7.21×10^{-5}	1.00×10^{-3}	2.50×10^{-2}	3.00×10^{3}	1.71×10^{3}
1.04×10^{0}	1.60×10^{-5}	4.79×10^{-5}	1.00×10^{-3}	1.67×10^{-2}	2.93×10^{3}	1.76×10^{3}
9.80×10^{-1}	4.81×10^{-5}	1.09×10^{-4}	7.50×10^{-4}	5.00×10^{-2}	2.62×10^{3}	1.30×10^{3}
9.75×10^{-1}	4.81×10^{-5}	2.19×10^{-4}	1.50×10^{-3}	5.00×10^{-2}	3.73×10^{3}	1.46×10^{3}
6.97×10^{-1}	4.81×10^{-5}	1.08×10^{-4}	1.00×10^{-3}	5.00×10^{-2}	3.11×10^{3}	1.40×10^{3}
1.43×10^{0}	4.81×10^{-5}	2.16×10^{-4}	1.00×10^{-3}	5.00×10^{-2}	3.07×10^{3}	1.38×10^{3}

4.2. Physics-Based Model: Acoustic Resonator

In order to fulfill the requirements of a hybrid approach we need first of all a physical equation to serve as a base. For this purpose we use one of the most well-known acoustical assets, the Helmholtz resonator. A Helmholtz Resonator is an acoustic system consisting of a cavity of volume *V* with a neck of length *l* and cross-sectional area *A*. When the acoustic frequency is sufficiently low so that the wavelength is much larger than the resonator's dimensions the compressible air in the system behaves as a mechanical mass-spring resonator, the compressible air acting as a spring while the air mass in the neck acts as a compact mass, for more information on acoustics modeling the reader can refer to [15,17–19]. In Figure 5 a Helmholtz Resonator is represented.
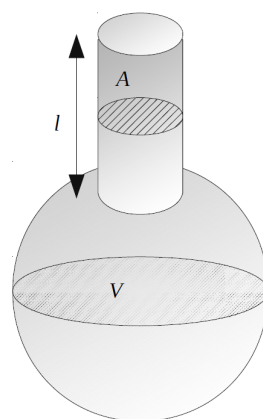

Figure 5. Design of a classic Helmholtz Resonator.

It is modeled by means of the resonance frequency Equation (2),

$$f_0 = \frac{c}{2\pi}\sqrt{\frac{A}{Vl}} \tag{2}$$

which is the frequency at which the system reaches the maximum oscillation amplitude generating the maximum dissipation, resulting this in its absorbed frequency. This equation is the one used for calculating the theoretical value of the resonance frequency values for the acoustic prototypes described in the previous section. Note that this model is built around strong hypothesis, so the use of a hybrid methodology is key to alleviate the impact of these hypothesis.

4.3. Regression Technique: Code2Vect

The second contribution concerns the data-driven model. A regression technique able to build a regression for the correction in the low-data limit is needed. For that purpose a recently developed technique presented in [20] will be used. This technique has been proven to perform well in the low data limit with accurate regression capabilities in different fields [21]. An extended overview of this technique can be found in Aappendix A. For the sake of completeness we briefly summarize it. Code2Vect maps data, eventually heterogeneous, discrete, categorical, ... into a vector space equipped of an euclidean metric allowing computing distances, and in which points with similar outputs remain close one another as sketched in Figure 6.

We assume that points in the origin space (space of representation or high-dimensional space) consist of P arrays composed on N entries. They are assumed arrays because they cannot be considered vectors, and are noted by $\mathbf{y}_i$. Their images in the vector space are noted by $\mathbf{x}_i \in \mathbb{R}^d$, with $d \ll N$, this time real vectors subjected to the rules of coordinate transformation. Regarding the choice of d, it is an user-defined parameter. However, it is important to keep in mind that the lower the parameter d is, the more non-linear the mapping has to be to place the points in accordance with a given target. Therefore, a balance should be kept between the richness of the interpolation basis and the pre-selected dimensionality of the reduced space. That vector space is equipped of the standard scalar product and the associated Euclidean distance. The mapping is described by the $d \times N$ matrix $\mathbf{W}$,

$$\mathbf{x} = \mathbf{W}\mathbf{y}, \tag{3}$$

where both, the components of $\mathbf{W}$ and the images $\mathbf{x}_i \in \mathbb{R}^d$, $i = 1, \cdots, \text{P}$, must be calculated. Each point $\mathbf{x}_i$ keeps the label, denoted by $\mathcal{O}_i$ (value of the output of interest, here assumed scalar), associated with its origin point $\mathbf{y}_i$.

We would like placing points $\mathbf{x}_i$, such that the Euclidean distance with any other point $\mathbf{x}_j$ scales with their outputs difference, i.e.,

$$(\mathbf{W}(\mathbf{y}_i - \mathbf{y}_j)) \cdot (\mathbf{W}(\mathbf{y}_i - \mathbf{y}_j)) = \|\mathbf{x}_i - \mathbf{x}_j\|^2 = \|\mathcal{O}_i - \mathcal{O}_j\|^2, \tag{4}$$

where the coordinates of one of the points can be arbitrarily chosen. Thus, there are $\frac{\text{P}^2}{2} - \text{P}$ relations to determine the $d \times N$.

The final goal is to use the Helmholtz equation to obtain the theoretical resonance frequency of the 23 samples and *Code2Vect* to model the correction between this theoretical resonance and the one measured in the acoustic bench. As before stated, *Code2Vect* is used for performing the regression of the deviation between the resonance frequency predicted by the physics-based model and the measured one.
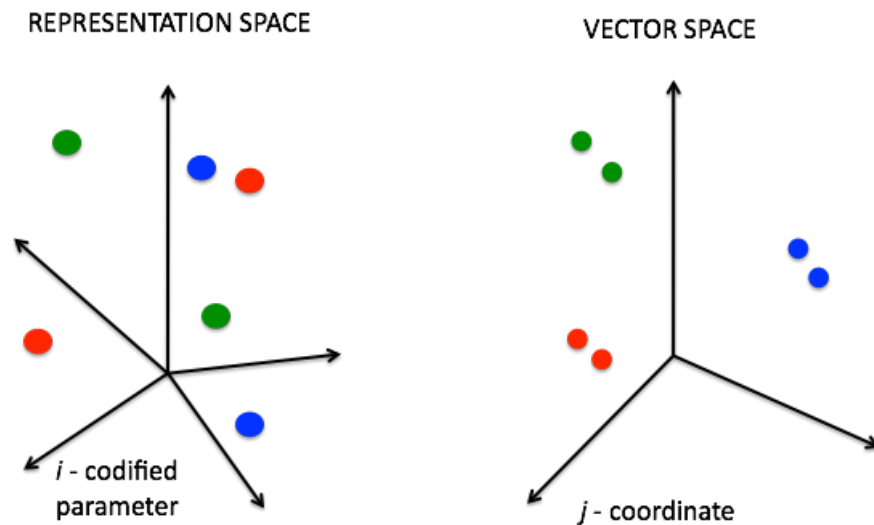
REPRESENTATION SPACE   VECTOR SPACE

i - codified parameter   *j* - coordinate

Figure 6. Input space(**left**) representing the input data $\mathbf{y}_i$ and vector space(**right**) representing the reduced coordinates $\mathbf{x}_i$.

5. Results

In this section two analysis will be performed, first a regression from a classical point of view, that is, a data-driven regression on the measured resonance frequency. Later, the regression will be performed on the correction as required for hybrid approaches. The accuracy of these two analysis will then be compared. The resonance frequency of a Helmholtz resonator depends on three parameters, as seen in Equation (2), length of the neck, area of the neck and volume of the cavity. The design parameters of the prototype that are considered equivalent are:

- The volume V of the cylindrical cavity.
- The open surface So represents the area of the neck, this parameter is the sum of the area of all the orifices in the cover, that are connected to the cavity.
- The thickness of the cover e is the length of the pipe.

These three parameters will be used to calculate the resonance frequency following Equation (2). Firstly, we will perform a data-driven approach in which a regression is built on the quantity of interest itself. *Code2Vec* will be applied to the data-set using 21 points as training data randomly chosen. For that purpose all the geometrical inputs considered in the design of experiments (diameter, height and volume of the cavity, open surface and thickness of the cover), 5 in total, are used to perform a regression on the measured resonance frequency. This data living in a 5 dimensional space is reduced to a 1 dimensional space, where each one of the 21 samples will be represented by one point. The obtained space is represented in Figure 7. Bottom right of the figure represents the reduced space where the value of the resonance frequency is used to color to each point. It can be appreciated how this space is correctly ordered according to the target. The following behaviors are observed:

- *Volume* has inverse relationship with the target: accordance with the preliminary model based on Helmholtz equation. This can be appreciated on how the cluster is ordered. The yellow color represents higher values of the normalized label and they appear in opposite position when coloring the cluster accordingly to the value of V.
- *Thickness* has inverse relationship: which is in accordance with the preliminary model.
- *POA* shows the same influence as *So* since $S_o = POA \cdot \pi \cdot (\frac{d}{2})^2$.
- *H*, shows the same behaviour as V since it is directly related to the volume, as $V = \pi r^2 H$ is the formula for the volume of a cylinder.
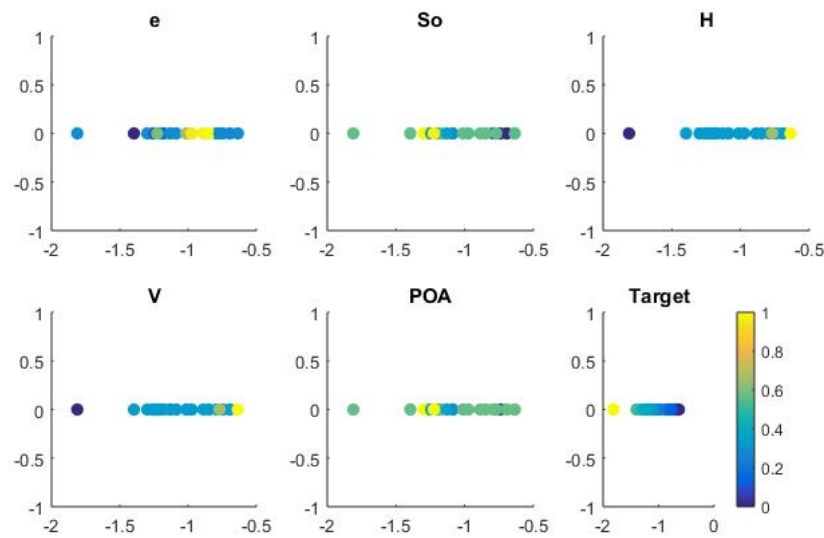
Figure 7. Reduced space after computing *Code*2*Vect* for cylindrical samples.

In the light of these results the input data may be reduced from 5 inputs to 3, removing *POA* and *H* from the case. In order to prove the guess right of this choice we perform the same analysis by *Code*2*Vect* using only *So*, *V* and *e* as inputs, which also coincide with the parameters used in Helmholtz equation. To check the accuracy we use 21 points to build the model, and the other two (randomly selected) are left outside. Once the model is built the two points are placed in the reduced space and their target value is interpolated resulting on a predicted value for the resonance frequency. In Figure 8 the predicted values vs. the real ones are compared. For both cases, one using 5 input parameters and another using 3 input parameters, prediction remains on the same order of magnitude on the checking points. It can be concluded that for this case it suffices to consider the three inputs present in the Helmholtz equation, area of the open surface (*So*), thickness of the cover (*e*) and volume of the cavity (*V*).
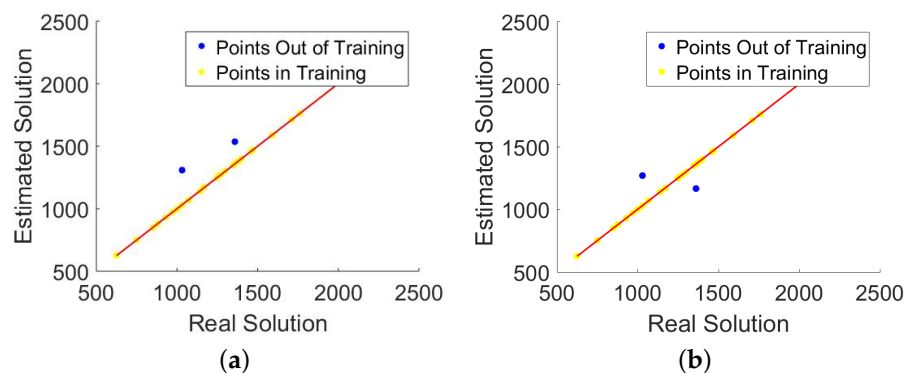
Figure 8. Data-driven prediction capabilities using 5 input parameters 5 (**a**) and 3 input parameters (**b**).

The next step is to perform the same analysis on the correction rather than directly in the resonance frequency. Theoretical resonance frequency is obtained by means of Equation (2). The values of this quantity of interest in both domains (theoretical and experimental) are represented in Figure 9a, that reveals the fact that tendencies are kept, however, the numerical values exhibit a gap. The ratio between both values is represented in Figure 9b. All the values being around 2 so it is proposed considering:

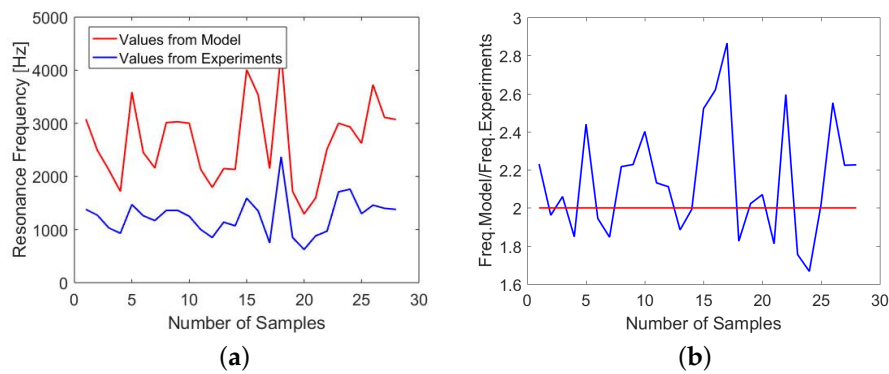$$\mathcal{F}_{r,data} = 2\mathcal{F}_{r,model} + C(V, e, S_o) \tag{5}$$

Figure 9. Theoretical and measured values of the resonance frequency (**a**), ratio between both values (**b**).

For testing the hybrid twin capabilities two randomly selected points are removed from the training data-set and the correction model regression is performed. Once the value of the correction for all the points (the ones in the training and the ones used for the regression) is obtained it is added to physics-based model affected by the scale factor just introduced. This will result on the new predicted resonance frequency. In Figure 10 results on the prediction of resonance target are displayed. Figure 10 on the left represents the estimated value of the resonance frequency obtained by a classical data-driven regression. Blue points are the ones used for training. Figure 10 on the right shows results on the hybrid twin predictions. It can be noticed how the choice of the hybrid twin approach improves the predictions accuracy. This superiority can be explained by the fact that, the model is richer because the non-linearities are represented by the physics-based model and thus the regression on the correction is more precise because the gap is much less nonlinear.
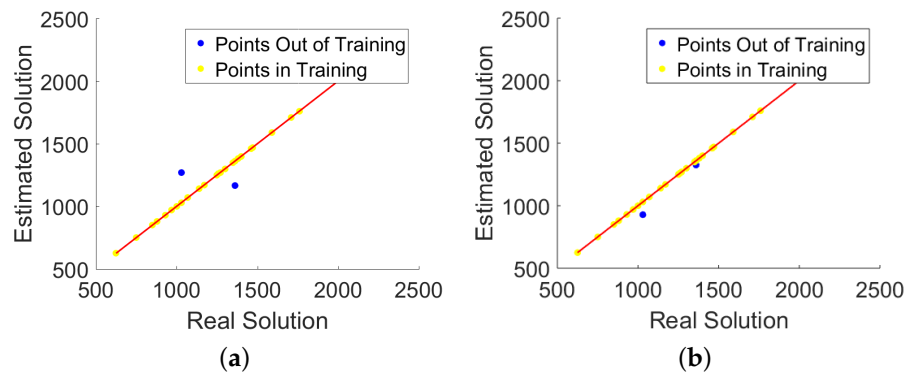

Figure 10. Prediction capabilities for data-driven (**a**) and Hybrid Twin (**b**) approaches.

6. Conclusions

This work proved the benefits of the Hybrid Twin approach for modeling new acoustical prototypes. Taking advantage of knowledge kept in physical equations, specifically Helmholtz equation, we proposed to build up a regression on the correction between the quantity of interest obtained by this ground-level model and real value experimentally measured. We proved that this approach provides more accurate results than strictly data-driven approaches. The base-model allows to know how the resonance frequency is related to the input parameters V, S_o and e, by using a hybrid approach we take profit of this knowledge, only needing to model a correction.

When using the same data-set, the use of a hybrid approach rather than a fully data-driven approach leads to more accurate predictions at a lower cost. The last is due to the reduction of the number of points (or samples) required for achieving the same quality results .

This first study serves as a staring point in the development of new technologies in the framework of the industry 4.0, where data-driven and machine learning techniques are widely used. By combining wisdom shaped as a physics-based equation and advanced machine learning techniques performed on data we embrace the benefits of both, physics-based and model-based approaches.

Author Contributions: C.A.M. is the main author responsible for performing the calculations of the Hybdrid Twin methodology and the data driven approach. A.C.M. was in charge of the acoustical analysis of the prototypes. O.S. performed the experimental measurements at the laboratory. E.P. and M.P. were in charge of supervising the development of the Hybrid Twin aproach for industrial prototypes. L.R. was in charge of supervising the acoustic approach and A.B. and F.C. were the supervisors of the whole Hybrid Twin methodology development. All authors have read and agreed to the published version of the manuscript.

Conflicts of Interest: The authors declare no conflict of interest.

Appendix A. Code2Vect

This appendix is aims at describing the development of the non-linear resolution of the Code2Vect. To solve the non-linearity in Equation (4) we propose a Newton-Raphson iteration scheme. By denoting $\mathbf{W}_i = \mathbf{W}(\mathbf{y}_i)$, the Newton at iteration reads n

$$\mathbf{W}_{n+1,i} = \mathbf{W}_{n,i} + \Delta\mathbf{W}_i, \tag{A1}$$

that replaced in the nonlinear counterpart of Equation (4)

$$(\mathbf{W}_i\mathbf{y}_i - \mathbf{W}_j\mathbf{y}_j) \cdot (\mathbf{W}_i\mathbf{y}_i - \mathbf{W}_j\mathbf{y}_j) = \|\mathbf{x}_i - \mathbf{x}_j\|^2 = \|\mathcal{O}_i - \mathcal{O}_j\|^2, \tag{A2}$$

the left hand member reads

$$\begin{aligned}
&(\mathbf{y}_i^T(\mathbf{W}_{n,i}^T + \Delta\mathbf{W}_i^T) - \mathbf{y}_j^T(\mathbf{W}_{n,j}^T + \Delta\mathbf{W}_j^T))((\mathbf{W}_{n,i} + \Delta\mathbf{W}_i)\mathbf{y}_i - (\mathbf{W}_{n,j} + \Delta\mathbf{W}_j)\mathbf{y}_j) = \\
&\mathbf{y}_i^T(\mathbf{W}_{n,i}^T + \Delta\mathbf{W}_i^T)(\mathbf{W}_{n,i} + \Delta\mathbf{W}_i)\mathbf{y}_i + \mathbf{y}_j^T(\mathbf{W}_{n,j}^T + \Delta\mathbf{W}_j^T)(\mathbf{W}_{n,j} + \Delta\mathbf{W}_j)\mathbf{y}_j - \\
&2\mathbf{y}_j^T(\mathbf{W}_{n,j}^T + \Delta\mathbf{W}_j^T)(\mathbf{W}_{n,i} + \Delta\mathbf{W}_i)\mathbf{y}_i.
\end{aligned} \tag{A3}$$

Since each term appearing the previous equation, presents the same structure, we can write the linearization for one of these terms:

$$\mathbf{y}_j^T(\mathbf{W}_{n,j}^T + \Delta\mathbf{W}_j^T)(\mathbf{W}_{n,i} + \Delta\mathbf{W}_i)\mathbf{y}_i \approx \mathbf{y}_j^T\mathbf{W}_{n,j}^T\mathbf{W}_{n,i}\mathbf{y}_i + \mathbf{y}_j^T\mathbf{W}_{n,j}^T\Delta\mathbf{W}_i\mathbf{y}_i + \mathbf{y}_i^T\mathbf{W}_{n,i}^T\Delta\mathbf{W}_j\mathbf{y}_j, \tag{A4}$$

and similarly for the other terms in Equation (A3).

The incremental counterpart of the transfer function at a given point is approximated as shown in Equation (A5)

$$\Delta\mathbf{W}_i = \sum_{k=1}^K \mathbb{A}_k \mathcal{P}_k(\mathbf{y}_i) \tag{A5}$$

where K is the number of terms in the approximation, $\mathcal{P}_k$ is the $k-th$ interpolation function and $\mathbb{A}_k$ is a matrix consistent with the structure of the transfer function. Once the increment is computed it is added to the previous state of the transfer function, $\mathbf{W}_{n,i}$.

$$\mathbf{W}_{n,i} = \sum_{j=1}^n \sum_{k=1}^K \mathbb{A}_k^j \mathcal{P}_k(\mathbf{y}_i) \tag{A6}$$

We have experienced that the number of interpolation functions (K) needed to consistent with the number training data. We have used K-Means clustering in order to locate smartly the position of the centroids in our input space (y), like that shape functions are likely centered in areas where we have more point concentration. For addressing the nonlinear approximation, radial basis interpolation was retained using either the gaussian or the inverse-quadratic radial kernels, both making use of the distance r

$$r_k = ||\mathbf{y} - \mathbf{y}_k||, \tag{A7}$$

from which both interpolants read

$$\mathcal{P}_k(r) = e^{-(\epsilon r_k)^2}, \tag{A8}$$

and

$$\mathcal{P}_k(r) = \frac{1}{\sqrt{1 + e^{-(\epsilon r_k)^2}}}, \tag{A9}$$

with ϵ affecting the shape of the radial kernel. Notwithstanding as it was said before, any other kind of interpolation function could be used in this methodology. Technically speaking, we do not have to reinforce continuity constraints as the problem do not involve any partial derivative.

References

1. Airports Commission: Final Report. Technical Report. 2015. Available online: https://www.gov.uk/government/publications/airports-commission-final-report (accessed on 12 October 2020).
2. Zhao, D. Transmission Loss Analysis of Parallel-Coupled Helmholtz Resonator Network. *JAIAA J.* **2012**, *50*. [CrossRef]
3. Sanada, A.; Tanaka, N. Extension of the frequency range of resonant sound absorbers using two-degree-of-freedom Helmholtz-based resonators with a flexible panel. *Appl. Acoust.* **2013**, *74*, 509. [CrossRef]
4. Paiva, R.C.D.; Valimaki, V. The Helmholtz Resonator Tree. In Proceedings of the 15th International Conference on Digital Audio Effects Conference (DAFx-12), York, UK, 17–21 September 2012.
5. Pascual, J.B. A Study of the Viscous Effects over an Acosutic Liner Using the Linearised Navier-Stokes Equations in Frequency Domain. In Proceedings of the 23rd AIAA/CEAS Aeroacoustics Conference, Denver, Colorado, 5–9 June 2017.
6. Piot, E. Mathematical tools for impedance models of sound-absorbing materials in aeronautics. In Proceedings of the Conference in honor of Abderrahmane Bendali, Pau, France, 12–14 December 2017.
7. Coyette, J.P.; Detandt, Y.; Lielens, G. Computational tools for modeling acoustic liners and propagation: Review of some key ingredients and challegnges. In Proceedings of the 15th CEAS-ASC Workshop1st Scientific Workshop of X-NOISE EV Acoustic Liners and Associated Propagation TechniquesEPFL, Lausanne, Switzerland, 13–14 October 2011.
8. Pascal, L.; Piot, E.; Casalis, G. A New implementation of the Extended Helmholtz Resonator Acoustic Liner Impedance Model in Time Domain CAA. *J. Comput. Acoust.* **2016**, *24*. [CrossRef]
9. Troian, R.; Dragna, D.; Bailly, C.; Galland, M.A. Broadband liner impedance eduction for multimodal aocustic propagation in the presence of a mean flow. In Proceedings of the AIAA/CEAS Aeroacoustics Conference, Lyon, France, 30 May–1 June 2016.
10. Sugimoto, R.; Astley, R.J.; Murray, P.B. Low frequency liners for turbofan engines. In Proceedings of the 20th International Congress on Acoustics, ICA 2010, Sydney, Australia, 23–27 August 2010.
11. Etaix, N.; Crawford, K.; Voisey, R.; Hopper, H. Redesigning Helmholtz resonators to achieve attenuation at multiple frequencies. In Proceedings of the 22nd International Congress on Acoustics, Buenos Aires, Argentina, 5–9 September 2016.
12. Piot, E.; Brazier, J.P.; Simon, F.; Fascio, V.; Peyret, C.; Ingenito, J. Design, manufacturing and demonstration of acoustic liners for air conditioning systems. In Proceedings of the 22nd AIAA/CEAS Aeroacoustics Conference, Lyon, France, 30 May–1 June 2016.
13. Spillere, A.; Reis, D.; Cordioli, J.A. A systematic review of semi-empirical acoustic liner models under grazing flow and high SPL. In Proceedings of the 22nd International Congress on Acoustics, Buenos Aires, Argentina, 5–9 September 2016.

14. Guess, A.W. Calculation of perforated plate liner parameters from specified acoustic and reactance. *J. Sound Vib.* **1975**, *40*, 119–137. [CrossRef]

15. Sommerfeldt, S.D.; Calton, M.F. Modeling acoustic resonators: From theory to application. In Proceedings of the Inter-Noise Conference, San Francisco, CA, USA, 9–12 August 2015.

16. ISO. Acoustics, Determination of sound absorption coefficient and impedance in impedance tubes. reactance. In *ISO Normative ISO10534-2*; ISO: Geneva, Switzerland, 1998.

17. Avraham Hirschberg. *Introduction to Aero-Acoustics of Internal Flows*; Von Karman Institute for Fluid Dynamics: Sint-Genesius-Rode, Belgium, 2020.

18. Rossing, T.D. *Handbook of Acoustics*; Springer: Berlin/Heidelberg, Germany, 2007.

19. Miyara, F. Introduccion a la Electroacustica. 2003. Available online: https://www.apuntesdeelectronica.com/audio/introduccion-a-la-electroacustica.htm (accessed on 12 October 2020).

20. Argerich-Martin, C.; Iba nez-Pinillo, R.; Barasinski, A.; Chinesta, F. Code2vect: An efficient heterogenous data classier and nonlinear regression technique. *Comptes Rendus Mec.* **2019**, *347*, 754–761. [CrossRef]

21. Yun, M.; Argerich, C.; Cueto, E.; Duval, J.L.; Chinesta, F. Nonlinear Regression Operating on Microstructures Described from Topological Data Analysis for the Real-Time Prediction of Effective Properties. *Materials* **2020**, *13*, 2335. [CrossRef] [PubMed]